Trihydroxynaphthalene Reductase from *Magnaporthe grisea*: Realization of an Active Center Inhibitor and Elucidation of the Kinetic Mechanism

James E. Thompson,[‡] Gregory S. Basarab,[‡] Arnold Andersson,[§] Ylva Lindqvist,[||] and Douglas B. Jordan*[,‡]

E. I. DuPont de Nemours Agricultural Products, Stine-Haskell Research Center, Newark, Delaware 19714, Department of Molecular Biology, Swedish University of Agricultural Sciences, Uppsala Biomedical Center, S-75124 Uppsala, Sweden, and Division of Structural Biology, Department of Medical Biochemistry and Biophysics, Karolinska Institute, S-171 77 Stockholm, Sweden

Received September 18, 1996; Revised Manuscript Received November 22, 1996[⊗]

ABSTRACT: Active trihydroxynaphthalene reductase (3HNR) is essential for the biosynthesis of fungal melanin by *Magnaporthe grisea* and is a focus of inhibitor design studies directed toward control of blast disease in rice. Tricyclazole, a preventative fungicide against rice blast, has been previously characterized as inhibiting 3HNR noncompetitively [Viviani, F., Vors, J. P., Gaudry, M., & Marquet, A. (1993) *Bull. Soc. Chem. Fr. 136,* 395−404] with respect to its naphthol substrate. Our steady-state kinetic and fluorescence titration studies show that instead the inhibitor binds competitively with respect to the naphthol substrate and that it binds to 3HNR forms with the preferences 3HNR·NADPH > 3HNR·$NADP^+$ > 3HNR (unliganded); K_i = 15 nM, 0.56 μM, and K_d = 8.5 μM, respectively. Analysis of the frontier molecular orbitals of tricyclazole and NADP(H) provides a basis for the affinity differences of tricyclazole for 3HNR·NADP(H) enzyme forms. Fluorescence titrations show that NADPH and naphthol substrates form binary complexes with 3HNR [K_d($NADP^+$) = 38 μM and K_d(U7278, an alternate naphthol-like substrate) = 220 μM]. However, the overwhelmingly preferred order of productive binding is NADPH followed by naphthol substrate, as shown by the uncompetitive inhibition of 3HNR by tricyclazole with respect to NADPH. Consistent with this mechanism, the K_m's for the naphthol substrates U7278 and scytalone (5 and 6 μM, respectively) are much lower than the K_d's of the binary complexes. The partition ratio of U7278 and a physiological substrate (scytalone) was 95:1 and unchanged on varying 3HNR·$NADP^+$/3HNR(unliganded), which is also consistent with the ordered mechanism. The pH dependence of the hydride transfer rate from U7278 to $NADP^+$ was measured, as was the pH dependence of k_{cat}/K_m ($NADP^+$). Hydride transfer had a pH dependence which suggests a single deprotonated residue (pK_a = 6.0) is required for catalysis. k_{hyd}, the rate constant for hydride transfer, was 9-fold larger than k_{cat} with U7278 as a substrate. A burst in the pre-steady-state suggests that release of one or both of the products is rate limiting to k_{cat} at pH 7.0. The pH dependence of k_{cat}/K_m($NADP^+$) indicates a requirement for a single deprotonated group and this ionization is assigned to the 2′ phosphate of $NADP^+$. 3HNR was found to be 800-fold more specific for $NADP^+$ relative to NAD^+. Analysis of sequence and structure [Andersson, A., Jordan, D. B., Schneider, G., & Lindqvist, Y. (1996) *Structure 4,* 1161−1170] reveals that 3HNR is a member of the short-chain dehydrogenase superfamily of enzymes.

In order for the fungus *Magnaporthe grisea* to initiate blast disease in rice, it must melanize an infection structure (the appresorium) (Howard & Ferrari, 1989). Consequently, the enzymes of the melanin biosynthetic pathway in *M. grisea* are biochemical targets for the design of antipenetrant fungicides. The fungal melanin biosynthesis pathway (Figure 1) includes a series of successive reductions and dehydrations from 1,3,6,8-tetrahydroxynaphthalene to 1,8-dihydroxynaphthalene, the last identified precursor of fungal melanin. Trihydroxynaphthalene reductase (3HNR)[1] catalyzes the second reduction of the pathway, a NADPH dependent reduction of the presumed keto tautomer of 1,3,8-trihydroxynaphthalene to yield vermelone. *In vitro,* 3HNR is capable of catalyzing reduction of the pathway precursor, 1,3,6,8-tetrahydroxynaphthalene, to scytalone. Other naphthol-like substrates have also been identified (Figure 2). 3HNR also catalyzes the scytalone dehydratase reaction, albeit very poorly (Figure 2). The stereochemistry of the enzymatically catalyzed reaction has been shown experimentally to involve transfer of the *pro-S* hydrogen from C-4 of the nicotinamide ring to the *si* face of the naphthol substrate (Figure 3) (Viviani *et al.,* 1991).

Spontaneous genetic knockouts of 3HNR were identified in *M. grisea* on the basis of the accumulation of metabolites derived from trihydroxynaphthalene. These mutants have been shown to be non-pathogenic to rice (Chumley & Valent,

* To whom correspondence should be addressed at Stine-Haskell Research Center, Building 300, 1094 Elkton Road, Newark, DE 19714. Tel: (302) 451-0075. FAX: (302) 366-5738. E-mail: jordandb@esvax.dnet.dupont.com.

[‡] E. I. DuPont de Nemours Agricultural Products.

[§] Swedish University of Agricultural Sciences.

[||] Karolinska Institute.

[⊗] Abstract published in *Advance ACS Abstracts,* February 1, 1997.

[1] Abbreviations: $\Delta\epsilon$, change in extinction coefficient; 3HN, 1,3,8-trihydroxynaphthalene; 3HNR, trihydroxynaphthalene reductase; MES, morpholinoethanesulfonic acid; Tris, trihydroxyaminomethane; MTEN, 50 mM MES, 25 mM Tris, 25 mM ethanolamine, 100 mM NaCl; PQ, 9,10-phenanthrenequinone; U7278, 2,3-dihydro-2,5-dihydroxy-4*H*-benzopyran-4-one; tricyclazole, 5-methyl-1,2,4-triazole-(3,4-*b*)-benzothiazole; SD, scytalone dehydratase; k_{hyd}, rate constant for hydride transfer; 4HN, 1,3,6,8-tetrahydroxynaphthalene.

S0006-2960(96)02355-0 CCC: $14.00

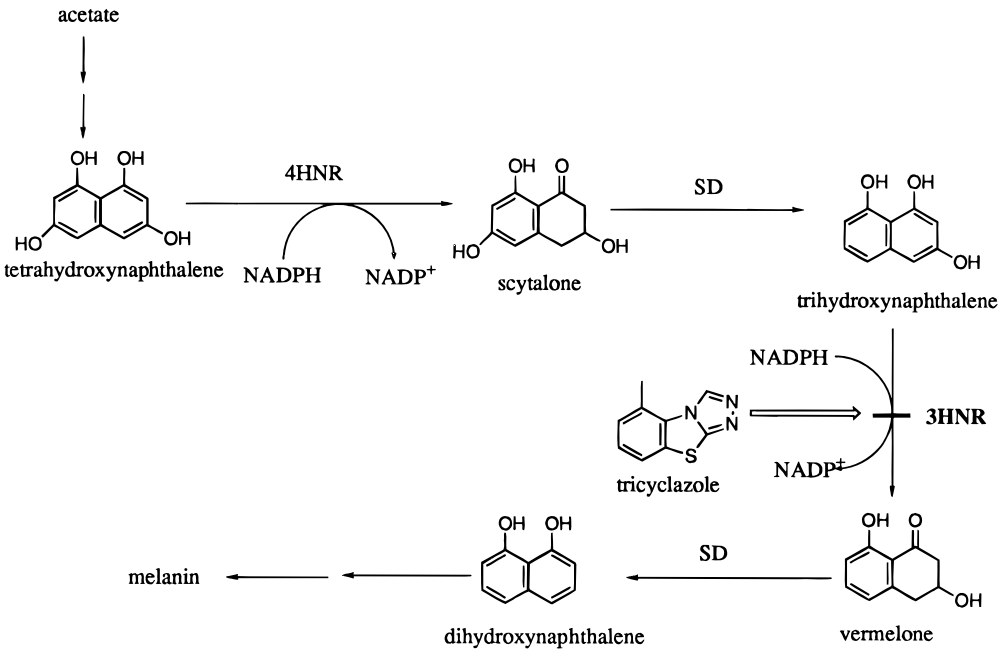

FIGURE 1: Fungal melanin biosynthetic pathway. 4HNR, tetrahydroxynaphthalene reductase; SD, scytalone dehydratase; 3HNR, trihydroxynaphthalene reductase. Tricyclazole stops the pathway at the thick line, leading to the accumulation of trihydroxynaphthalene and its oxidized derivatives.

1990). The melanin biosynthetic metabolites that accumulate in *M. grisea* grown in the presence of the antipenetrant fungicide tricyclazole (Figure 1) are the same as those found in the *M. grisea buf*$^-$ mutants lacking 3HNR (Jordan, unpublished results). Tricyclazole was shown to inhibit the 3HNR-catalyzed reduction of tetrahydroxynaphthalene, and a multi-site model for tricyclazole binding was proposed (Viviani *et al.*, 1993). However, such a model is inconsistent with the structure of the 3HNR·tricyclazole·NADPH ternary complex, recently solved by X-ray diffraction methods (Andersson *et al.*, 1996a). In this complex the *pro-S* hydrogen of the nicotinamide ring is pointed toward the centroid of the azole ring of the inhibitor at a distance within 2 Å.

The physiological substrate for 3HNR, 1,3,6-trihydroxynaphthalene, is unstable in an aerobic environment where it rapidly undergoes condensations and oxidation to 2-hydroxyjugulone (Wheeler, 1982). We report here the steady-state kinetic parameters for a natural substrate (scytalone) and two alternate substrates (U7278 and phenanthrenequinone). The results from steady-state kinetic studies allow determination of the kinetic mechanism and measurement of the specificity of 3HNR for these subtrates. Our results from inhibition and equilibrium binding studies reconcile the structural and kinetic data for the 3HNR·tricyclazole·NADPH complex and require revision of the multi-site model for the inhibition of 3HNR by tricyclazole. The inhibition and binding studies also reveal significant modulations in affinity of tricyclazole for 3HNR depending on the NADP(H) cofactor. We have also used pre-steady-state kinetic measurements to provide information about the rate limiting steps during catalysis by 3HNR.

MATERIALS AND METHODS

Materials and General Methods. 3HNR was cloned, expressed, and purified as described previously (Andersson *et al.*, 1996b). U7278 was synthesized as described elsewhere (J. E. Thompson, G. S. Basarab, and D. B. Jordan, in preparation). Tricyclazole was from Chemical Service (West Chester, PA). Beef heart glutamate dehydrogenase was from Boehringer Mannheim (Indianapolis, IN). All other materials were from Aldrich Chemical (Milwaukee, WI) or Sigma Chemical (St. Louis, MO). Unless otherwise noted, nonlinear least-squares analysis was carried out using the computer program RS1 (BBN Research Systems; Cambridge, MA). Scytalone was purified from cultures of *rsy*$^-$ mutants of *M. grisea* (Chumley & Valent, 1990; Thompson *et al.*, 1996).

Spectrophotometric Methods. Spectrophotometric properties were measured by using an HP 8542A diode array spectrophotometer (Hewlett Packard). All enzyme assays, except those involving phenanthrenequinone (PQ), were carried out in 50 mM MES, 25 mM Tris, 25 mM ethanolamine, 100 mM sodium chloride (MTEN) at 25 °C, and the ionic strength at a given pH was adjusted with NaCl to $I = 0.19$. Assays with PQ were in 100 mM phosphate buffer, pH 7.0, 5% DMSO, and 25 °C. This concentration of DMSO was required for solubility of PQ and did not affect enzyme activity (data not shown). U7278 oxidation was assessed by continuously measuring the absorbance of the reaction mixture at 340 nm. The net $\Delta\epsilon_{340}$ for oxidation of U7278 by $NADP^+$ is 4.5 mM^{-1} cm^{-1}. This $\Delta\epsilon_{340}$ was found to apply at all pH's studied. The ϵ_{280} for 3HNR was calculated to be 20.76 mM^{-1} cm^{-1} using the Peptidesort computer program of the Wisconsin Sequence Analysis Package (Genetics Computing Group, 1994).

Oxidation of scytalone was monitored at 355 nm in the presence of 2.5 mM α-ketoglutarate and 400 μg of glutamate dehydrogenase in MTEN buffer containing 0.1 M ammonium chloride instead of 0.1 M sodium chloride. The glutamate dehydrogenase couple recycles product NADPH to $NADP^+$. The net $\Delta\epsilon_{355}$ for oxidation of scytalone under these conditions is 5.3 mM^{-1} cm^{-1}.

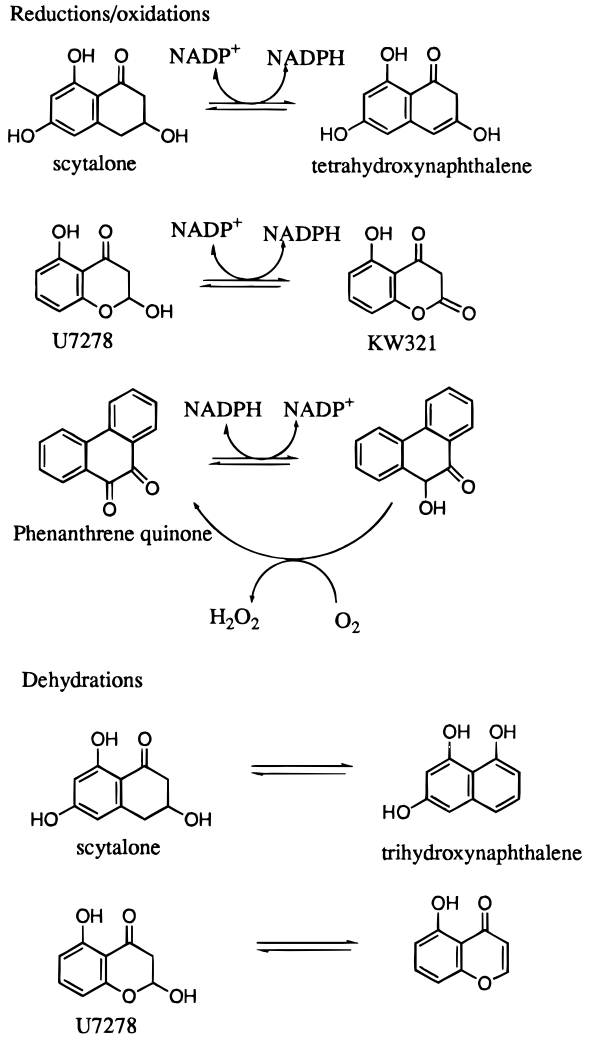

FIGURE 2: Chemical transformations catalyzed by 3HNR referred to in this work.

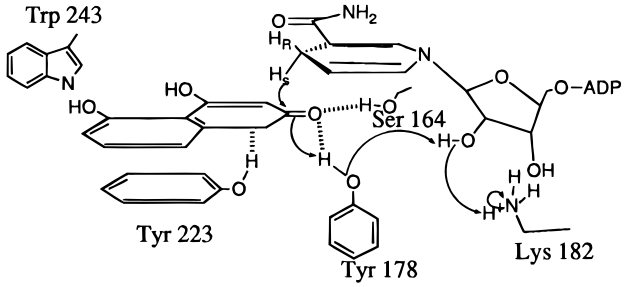

FIGURE 3: Putative mechanism for trihydroxynaphthalene reduction. The stereochemistry of the reduction is as shown (Viviani *et al.*, 1993). The interactions of the side chains with the substrate were inferred by modeling trihydroxynaphthalene in the active site of 3HNR (Andersson *et al.*, 1996a) using the computer program Sybyl (Tripos, St. Louis, Mo).

Reduction of PQ by NADPH catalyzed by 3HNR was monitored at 340 nm and $\Delta\epsilon_{340} = -6.2$ mM^{-1} cm^{-1}. Reduced PQ autoxidizes back to PQ rapidly on the experimental time scale (data not shown), and so the concentration of PQ does not change during the course of an assay.

Steady-state kinetic parameters were determined by fitting initial velocity data to eq 1 using the Kinetasyst computer program (IntelliKinetics; Princeton, NJ). Concentrations of both naphthol and nucleotide were varied when U7278 and PQ were substrates, the concentration of NADP$^+$ was held at 0.25 mM when scytalone was the substrate. Equation 1 describes ordered, sequential addition of substrates (Segel, 1975):

$$\nu = \frac{VAB}{K_{ia}K_b + K_aB + K_bA + AB} \quad (1)$$

where ν is initial velocity, V is maximum velocity, A is the concentration of the substrate binding first (NADP(H)), and B is the concentration of the substrate binding second (naphthol), K_{ia} is the dissociation constant of substrate A, K_b is the Michaelis constant for substrate B, K_a is the Michaelis constant for substrate A. When only one substrate is varied, eq 1 can be simplified to $\nu = VA/(K_a + A)$.

The scytalone dehydratase activity of 3HNR was measured by monitoring the dehydration of scytalone and U7278 in the presence of 3HNR but in the absence of NADP$^+$. $\Delta\epsilon_{352} = 4.1$ mM^{-1} cm^{-1} for the dehydration of scytalone and $\Delta\epsilon_{320} = 1.5$ mM^{-1} cm^{-1} for dehydration of U7278. The dehydration catalyzed by 3HNR is sufficiently slow (a rate of 0.1 μM/min is typical) that the nonenzymatic rate of dehydration was subtracted from the net rate observed with enzyme present to obtain the rate with enzyme alone. Enzymatic rates were always at least 3-fold faster than the background rates. The data were fitted to $\nu = VA/(K_a + A)$ for scytalone or $\nu = VA/(K_a + A + A^2/K_{ia})$ for U7278, as some substrate inhibition was observed.

pH independent parameters and pK_a's were obtained by fitting the rate constant for hydride transfer, k_{hyd}, and k_{cat}/K_m(NADP$^+$) as function of pH to eq 2, which describes the titration of a single ionizable group (Segel, 1975):

$$k_{cat}/K_m = \overline{k_{cat}/K_m}(1 + [H^+]/K_a)^{-1} \quad (2)$$

where $\overline{k_{cat}/K_m}$ is the pH independent k_{cat}/K_m and K_a is the acid dissociation constant for the group affecting catalysis. k_{hyd} may be substituted for k_{cat}/K_m in eq 2.

Inhibition Studies. Tricyclazole inhibition of scytalone oxidation and PQ reduction catalyzed by 3HNR was measured by assaying the reactions as described above, in the presence of varying concentrations of tricyclazole. In both cases, the amount of inhibitor was comparable to the concentration of enzyme present, and the total tricyclazole concentration could not be assumed to equal that of free tricyclazole. The equation describing competitive inhibition (Segel, 1975) was modified to reflect this, yielding eq 3

$$\nu = VS/\{S + K_m[1 + [I_T - (K_i + E_{T,app} + I_T - \sqrt{(K_i + E_{T,app} + I_T)^2 - 4E_{T,app}I_T})/2]/K_i]\} \quad (3)$$

where

$$E_{T,app} = E_T - E_T\left(1 + \frac{S}{K_m}\right)$$

and where ν is initial velocity, V is maximum velocity, S is substrate concentration, I_T is total inhibitor concentration, E_T is total enzyme concentration, K_i is the dissociation constant for the inhibitor, K_m is the Michaelis constant for the substrate and I_T is total inhibitor concentration. Initial velocity data was measured as a function of substrate at different concentrations of tricyclazole, and the data were fit to eq 3 to obtain K_i.

When tricyclazole inhibition of PQ reduction was measured as a function of NADPH concentration, the data were fit to eq 4 which describes uncompetitive inhibition (Segel, 1975); the variable definitions are the same as for eq 3. Total tricyclazole could be equated with free tricyclazole in this case, as PQ was maintained at 4 times K_m and [3HNR] was maintained 3-fold lower than the lowest tricyclazole concentration. NADPH ranged from 15 to 60 μM.

$$v = \frac{VS}{K_m + S(1 + (I_T/K_i))} \quad (4)$$

Fluorescence Titrations. Fluorescence of 3HNR was measured as a function of ligand concentration on an SLM8000 fluorimeter (SLM/Aminco, Champaign−Urbana, IL). All titrations were performed in MTEN buffer, pH 7.0 at 25 °C. 3HNR fluorescence (excitation at 295 nm, emission at 340 nm) was measured as a function of added ligand. Corrections for absorption of light by added ligands were determined by measuring the fluorescence of tryptophan (0.1 mM) as a function of ligand concentration, fitting the data to a single exponential and correcting the 3HNR data accordingly. To obtain the dissociation constant, K_d, the corrected fluorescence data were fit to eq 5 (Birdsall *et al.*, 1980),

$$F_{obs} = F_o - (F_o - F_\infty)[(K_d + E_T + L_T - \sqrt{(K_d + E_T + L_T)^2 - 4E_TL_T})/2E_T] \quad (5)$$

where F_{obs} is the observed fluorescence, F_o is the fluorescence in the absence of ligand, F_∞ is the fluorescence at infinite ligand concentration, E_T is the total enzyme concentration, and L_T is the total ligand concentration.

Measurement of Equilibrium Constants for Scytalone Oxidation and PQ Reduction. The equilibrium constant for scytalone oxidation was measured by allowing a reaction containing 0.1 mM $NADP^+$, 0.1 mM scytalone, and 3HNR to react to its end point. A $\Delta\epsilon_{348} = 9.41$ mM^{-1} cm^{-1} was used to measure the extent of reaction. 20 μM PQ was reduced with 0.1 mM NADPH under a N_2 atmosphere in the presence of glucose oxidase and catalase to insure anaerobic conditions. The $\Delta\epsilon_{340} = -8.5$ mM^{-1} cm^{-1} for the anaerobic reduction of PQ.

Methods for Computation of Frontier Molecular Orbitals. Full geometry optimizations were performed on a Silicon Graphics Indigo workstation using the semi-empirical MOPAC program (Dewar, 1983). The AM1 parameterization was employed for all calculations. $NADP^+$ and NADPH were truncated to the *N*-methylnicotinamide cation and the *N*-methyldihydronicotinamide ring respectively for the calculations. A charge of 0 was assigned to tricyclazole and *N*-methyldihydronicotinamide and of +1 for *N*-methylnicotinamide cation.

Measurement of Substrate Partitioning. The simultaneous oxidations of U7278 and scytalone were monitored at 244, 282, 294, 310, and 348 nm in MTEN buffer at pH 7.0 and 25 °C without the glutamate dehydrogenase couple. The concentration of scytalone was 0.2 mM and the concentration of U7278 was 15 μM during these experiments. $NADP^+$ was varied from 10 to 100 μM. The net changes in extinction coefficient on oxidation of scytalone and U7278 were ($\Delta\epsilon_\lambda^{substrate}$, all in $cm^{-1}mM^{-1}$): $\Delta\epsilon_{244}^{U7278} = 0.60$; $\Delta\epsilon_{244}^{scytalone} = 2.22$; $\Delta\epsilon_{282}^{U7278} = 3.86$; $\Delta\epsilon_{282}^{scytalone} = -2.70$; $\Delta\epsilon_{294}^{U7278} = 10.76$; $\Delta\epsilon_{294}^{scytalone} = -1.18$; $\Delta\epsilon_{310}^{U7278} = 10.2$; $\Delta\epsilon_{310}^{scytalone} = 1.0$; $\Delta\epsilon_{348}^{U7278} = 3.45$; and $\Delta\epsilon_{348}^{scytalone} = 9.41$. The net change in absorbance with time at any wavelength (ΔA_λ/min) is described by eq 6.

$$\Delta A_\lambda/\text{min} = \sum\left(\frac{\text{d[oxidized substrate]}}{\text{d}t}\right)\Delta\epsilon_\lambda^{substrate} \quad (6)$$

Equation 6 was solved simultaneously at the wavelengths listed using the computer program "$lineqs" in RS1 to extract the rates of oxidation of each substrate; the ratio of the rate of U7278 oxidation to the rate of scytalone oxidation is defined as the partition ratio Φ. Φ was measured in triplicate at each $NADP^+$ concentration.

Pre-Steady-State Kinetic Methods. Measurement of the rate of hydride transfer (k_{hyd}) was accomplished by rapid mixing of 3HNR and substrates to final concentrations of 100 μM 3HNR and 50 μM U7278 in MTEN buffer at various pH's. At each pH, the concentration of $NADP^+$ was adjusted upward until the measured rate no longer increased. 3HNR (200 μM) was held in one syringe while U7278 (100 μM) and $NADP^+$ (8.4, 2, 2, 0.8, 0.4, and 0.8 mM at pH's 5.4, 6, 6.5, 7, 8, and 9 respectively) were in the second syringe. The change in absorbance at 340 nm with time was monitored by using an Applied Photophysics (Leatherhead, U.K.) stopped-flow unit. The data were fit to $Ae^{-kt} + C$ to extract the first-order rate constant at each pH, and the measured k was regarded as k_{hyd}. At least three trials were averaged to obtain the reported values. pH independent k_{hyd} and the pK_a were obtained by fitting k_{hyd} as a function of pH to eq 2.

Measurement of the burst from the first turnover of U7278 and $NADP^+$ by U7278 was measured at 20 μM 3HNR, 50 μM U7278, 200 μM $NADP^+$. The reaction was monitored at 340 nm and the kinetic data were fit to eq 7 which describes a single exponential decay followed by a steady-state absorbance change.

$$\text{absorbance at 340 nm} = Ae^{-kt} + mt + b \quad (7)$$

A is the amplitude of the burst and k is the rate constant for the single exponential decay, t is time, m is the slope, and b is the y intercept of the steady-state portion of the reaction.

RESULTS AND DISCUSSION

Steady-State Kinetic Parameters. Initial velocities were measured as a function of substrate concentrations as described in materials and methods and are listed in Table 1. The directly measured substrate specificities are consistent with the physiological role of 3HNR. The k_{cat}/K_m for oxidation of U7278 is about 30-fold higher than that for scytalone. Scytalone has four exocyclic oxygens whereas U7278 has only three, and in this respect U7278 is more like the physiological substrate, 3HN. It is interesting to note that the K_m for all of the naphthol substrates are similar which suggests that little of the specificity shown by 3HNR is manifested in ground-state enzyme/substrate interactions.

The K_m's for $NADP^+$ and NADPH are also nearly identical, a finding in keeping with the dissociation constants for the 3HNR·NADPH and 3HNR·$NADP^+$ binary complexes (discussed later). The K_i's for $NADP^+$ and NADPH extracted from eq 1 are consistent with K_d's determined by fluorescence titration (Table 2). The errors are high for the

Table 1: Steady-State Kinetic Parameters for Reduction of Phenanthrenequinone and Oxidation of Scytalone and U7278 by 3HNR at pH 7.0

kinetic parameter	phenanthrenequinone	U7278	scytalone
k_{cat} (s^{-1})	13 ± 1	14 ± 2	0.38 ± 0.01
k_{cat}/K_m(naphthol) (M^{-1} s^{-1})	$(4.0 \pm 0.8) \times 10^6$	$(2.9 \pm 0.5) \times 10^6$ ($(5 \pm 1) \times 10^6$)[c]	$(5.6 \pm 0.9) \times 10^4$
K_m(naphthol) (μM)	3 ± 1	5 ± 3 (3 ± 1)[c]	6 ± 1
K_i[NADP(H)] (μM)	51 ± 28[a]	76 ± 76[b]	n/d
K_{eq}	10^{13} M^{-1} [d]	n/d	8×10^{-8} M
k_{cat}/K_m[NADP(H)] (M^{-1} s^{-1})	$(6.1 \pm 0.2) \times 10^5$ [a]	$(4.3 \pm 0.7) \times 10^5$ [b]	n/d
K_m[NADP(H)] (μM)	21 ± 6[a]	33 ± 8[b]	n/d

[a] NADPH. [b] NADP+. [c] Determined by partition analysis of scytalone and U7278 as described in Materials and Methods. [d] Calculated from the reduction potentials of NADPH and PQ (Naumann & Kayser, 1978). n/d, not determined.

Table 2: Dissociation Constants for Ligands and 3HNR at pH 7.0

ligand	K_d
$NADP^+$	38 ± 2 μM[a]
NADPH	31 ± 2 μM[a]
U7278	220 ± 20 μM[a] (150 ± 40 μM[b])
scytalone	1.4 ± 0.4 mM[b]
tricyclazole	8.5 ± 0.5 μM[a]

[a] Measured by fluorescence titration. [b] Measured as the K_m of the scytalone dehydratase reaction catalyzed by 3HNR.

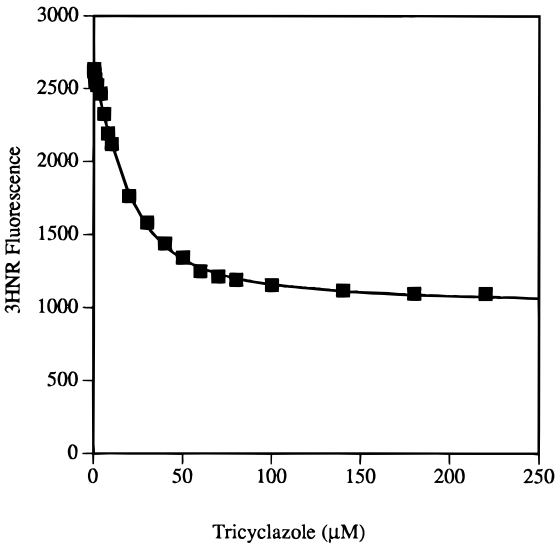

FIGURE 4: Titration of the fluorescence of 20 μM 3HNR with tricyclazole. The solid line shows the nonlinear least-squares fit to eq 5.

former values owing to the difficulty in obtaining initial velocities at concentrations of naphthol lower than K_m.

Dissociation Constants of Binary and Ternary Complexes. Dissociation constants of binary complexes were determined by measuring quenching of intrinsic protein fluorescence (the titration of 3HNR with tricyclazole is shown in Figure 4). The crystal structure of 3HNR·NADPH·tricyclazole (Andersson *et al.*, 1996b) shows that Trp243 is the likely fluorescence reporter. In the case of 3HNR·U7278, the K_d was measured two ways: by fluorescence titration and by measuring the K_m of the very poorly catalyzed ($k_{cat} = 0.001$ s^{-1}) dehydration reaction. The enzyme catalyzed dehydration rate is so slow under these conditions that the substrate binding to 3HNR may be safely assumed to reach equilibrium, and the K_m may regarded as K_d. The K_d for scytalone was determined in this manner as well, where k_{cat} (dehydration) for scytalone was 0.0002 s^{-1}. The dissociation constants for the binary complexes are reported in Table 2.

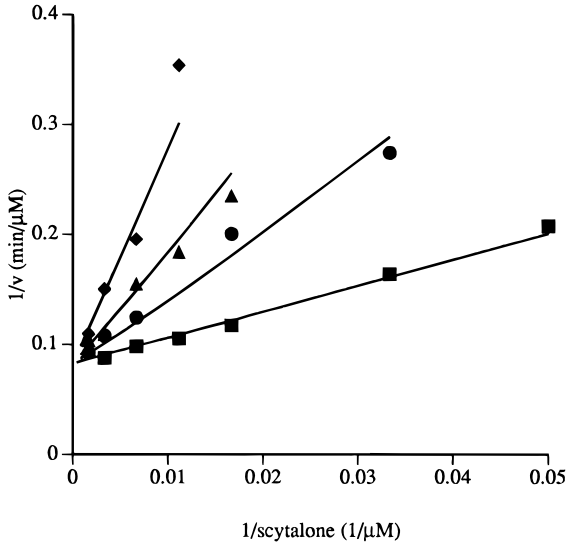

FIGURE 5: Inhibition of 3HNR catalyzed scytalone oxidation by tricyclazole. Tricyclazole = (■) 0 μM, (◆) 1 μM, (▲) 2 μM, and (○) 4 μM and [3HNR] = 0.69 μM. Reaction velocities were determined spectrophotometrically as in Materials and Methods and were fit to eq 3 (solid curves).

Dissociation constants for tricyclazole for the ternary complexes 3HNR·NADPH·tricyclazole and 3HNR·$NADP^+$·tricyclazole were determined by measuring initial velocities of scytalone oxidation and phenanthrenequinone reduction as a function of naphthol substrate and inhibitor concentrations at constant [NADP(H)]. The initial velocity data were fit to a model (eq 3) describing competitive inhibition (Figure 5). Although eq 3 describes a nonlinear relationship between reciprocal of initial velocity and reciprocal of substrate, in practice, the largest correction for binding of the inhibitor by enzyme was less than 15%, and so the best fit appears linear. Inhibition of PQ reduction by tricyclazole was also measured as a function of NADPH concentration and these data, which gave parallel lines in the double-reciprocal plots of $1/v$ vs 1/[NADPH] (data not shown), were fit to eq 4. Tricyclazole inhibits both oxidation and reduction competitively with respect to the naphthol substrate and inhibits reduction uncompetitively with respect to NADPH (Table 3).

The finding that tricyclazole is competitive with respect to naphthol substrates is consistent with the structure of the ternary complex solved by X-ray diffraction methods (Andersson *et al.*, 1996a) which shows that tricyclazole interacts with the *pro-S* C-4 hydrogen of the NADPH cofactor. Viviani and co-workers have shown that the *pro-S* hydrogen is the hydrogen transferred to substrate during reduction (Viviani *et al.*, 1992), and these results are not in dispute.

Table 3: Inhibition of 3HNR Activity by Tricyclazole at pH 7.0

varied substrate	inhibition type	K_i
phenanthrenequinone[a]	competitive	15 ± 3 nM
scytalone[b]	competitive	0.56 ± 0.05 μM
NADPH[c]	uncompetitive	8 ± 1 nM

[a] Measured at [NADPH] = 100 μM. [b] Measured at [$NADP^+$] = 100 μM. [c] Measured at [PQ] = 40 μM and corrected using K_m(PQ) = 3 μM (Table 1).

However, Viviani and co-workers previously investigated tricyclazole as an inhibitor of tetrahydroxynaphthalene (4HN) reduction by 3HNR (Viviani *et al.*, 1992) and concluded that tricyclazole was noncompetitive with respect to 4HN with K_i = 35 nM, but that azatricyclazole (K_i = 1.5 μM) was competitive with respect to 4HN. These results led to the proposal of a multi-site model for tricyclazole binding to 3HNR. However, in the experiments when noncompetitive inhibition was observed, the concentration of 3HNR was 90 nM (Viviani, 1990), greater than the studied concentrations of tricyclazole (30 and 60 nM). 4HN concentrations were less than 2-fold the K_m. Value errors in free tricyclazole concentration that result from these experimental conditions make straightforward determination of K_i and inhibition type impossible. The inhibition data of Viviani *et al.*, (1992) are consistent with the formation with a high-affinity 3HNR·NADPH·tricyclazole complex of nearly 1:1 3HNR:tricyclazole stoichiometry. The same experiments were performed at 0.25 mM NADPH, which is saturating (this work), and when 30 nM tricyclazole was added to assays including 90 nM enzyme, approximately 30% inhibition was observed (Viviani *et al.*, 1992).

Confirmation of a 1:1 3HNR:tricyclazole stoichiometry comes from titration of the active-site of 3HNR with tricyclazole (data not shown). At 200 nM 3HNR in the presence of 200 μM NADPH, the stoichiometry of tricyclazole:inactive enzyme was 0.90, as determined by measuring the 3HNR PQ reduction activity remaining after additions of tricyclazole and extrapolating the linear relationship to zero activity. Taken together, all available data support a model for tricyclazole binding to one site per 3HNR monomer with this site being the same as the site for naphthol substrate binding.

It is apparent from the K_d's of the binary and ternary complexes of tricyclazole with 3HNR that the binding of tricyclazole is modulated by the presence of the NADP(H) and by the oxidation state of the nicotinamide ring. Inhibition of scytalone oxidation and phenanthrenequinone reduction by tricyclazole was measured by a continuous spectrophotometric assay. Tricyclazole is bound 15-fold tighter to 3HNR·$NADP^+$ than to 3HNR(unliganded); in turn it is bound 37-fold tighter to 3HNR·NADPH than to 3HNR·$NADP^+$. In theory, the inhibition of PQ reduction by tricyclazole measured as a function of NADPH concentration should be noncompetitive as tricyclazole binds to both free 3HNR and 3HNR·NADPH. In practice, this is not observed because of the nearly 500-fold difference in the K_i's for the two complexes, and the observed inhibition with respect to NADPH is uncompetitive. Inhibition of 3HNR by tricyclazole is suggestive of a kinetic mechanism that is largely ordered sequentially with NADPH binding first and naphthol second. In other words, tight binding of tricyclazole is to the 3HNR·NADP(H) complex (as shown by uncompetitive inhibition of catalysis by tricyclazole with respect to NADPH) and tricyclazole inhibits catalysis competitively with respect to naphthol substrates; thus the naphthol substrates require the 3HNR·NADP(H) complex for tight binding.

Comparison of naphthol K_d's with their K_m's also supports the ordered sequential mechanism. 3HNR can form binary complexes with both $NADP^+$ and NADPH as well as with U7278 and scytalone. 3HNR does not show great preference for NADPH compared to $NADP^+$ (Table 2); the K_d's for the two complexes are essentially identical. This is not always true of dehydrogenases; dihydrofolate reductase has a 10^4-fold greater affinity for NADPH than for $NADP^+$ (Birdsall *et al.*, 1980). Although 3HNR is capable of binding U7278 and scytalone without cofactor present, the K_m's (5 and 6 μM) at saturating $NADP^+$ are much lower than the K_d's (220 and 1400 μM) of the 3HNR·naphthol complexes. Further evidence for this kinetic mechanism comes from the partitioning of scytalone and U7278 (discussed later).

Equilibrium Constant for Scytalone Oxidation and Stoichiometry of PQ Reduction. The measured equilibrium constant for scytalone oxidation is listed in Table 1. The concentrations of all reactants and products could be measured for the scytalone oxidation reaction, and the equilibrium constant for the reaction is 8×10^{-8} M^{-1}. This value is about 10-fold higher than that measured via the Haldane relationship (Viviani *et al.*, 1993). At equilibrium, the concentrations of reactants in the PQ reduction reaction are too low to be accurately determined. This is consistent with the value for the equilibrium constant calculated from the phenanthrenequinone reduction potential of 0.044 V (Naumann & Kayser, 1978), which yields a K_{eq} for reduction of 1×10^{13} M. Even at pH 7.0, the equilibrium favors products over reactants by 10^6.

The stoichiometry of PQ reduction was measured. With a 5-fold excess of NADPH, 1 equiv of NADPH (relative to PQ) was consumed. It is clear that although it is chemically possible to reduce both of PQ's carbonyls to alcohols, the second reduction is not observed with NADPH as the reductant. PQ may be regarded as a single reactant and product with regard to its 3HNR-catalyzed reduction with NADPH. The reduction of PQ has been often been used as an assay for dehydrogenases, particularly with regard to carcinogen metabolism [*e.g.*, Chung (1987), Klein (1992), and Torroren (1981)], but the stoichiometry of PQ reduction is seldom considered.

Computational Studies of Tricyclazole/NADP(H) Molecular Orbital Interactions. We examined the frontier molecular orbitals of NADPH and tricyclazole based on the positions of inhibitor and cofactor in the crystal structure (Andersson *et al.*, 1996) in an effort to understand the 36-fold increased affinity observed for tricyclazole binding to 3HNR·NADPH relative to 3HNR·$NADP^+$. We assumed that the orientation of the 3HNR·$NADP^+$·tricyclazole complex was similar to the 3HNR·NADPH·tricyclazole orientation and calculated the energy levels of the highest occupied molecular orbitals (HOMOs) and the lowest unoccupied molecular orbitals (LUMOs) for the NADP(H) nicotinamide rings and tricyclazole. The calculations were carried out in the gas phase, an approximation that should be reasonable, given that the crystal structure shows no solvent-exposed surface area for the nicotinamide ring or tricyclazole (Andersson *et al.*, 1996a). Table 4 summarizes the results.

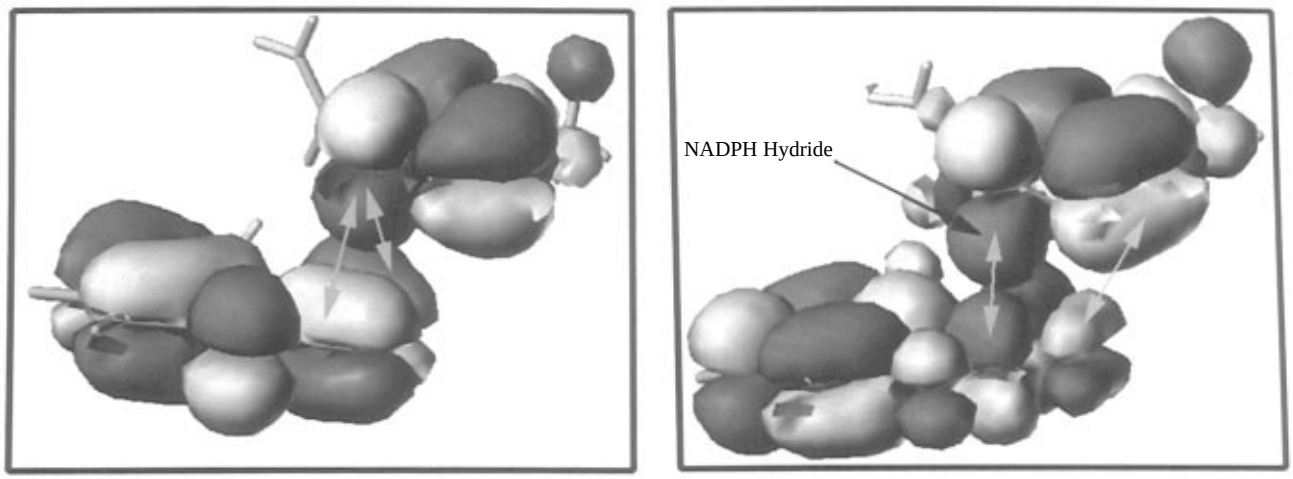

HOMO of Tricyclazole and LUMO of NADP $^+$ LUMO of Tricyclazole and HOMO of NADPH

FIGURE 6: Tricyclazole$_{HOMO}$/NADP(H)$_{LUMO}$ interactions. The figure was generated using the positioning of tricyclazole and cofactor found in the structure of the 3HNR·NADPH·tricyclazole ternary complex (Andersson *et al.*, 1996a).

Table 4: HOMO/LUMO Energy Gaps for Tricyclazole and NADP(H) When Bound to 3HNR

molecular orbital interaction	HOMO/LUMO gap [eV (kcal/mol)]
tricyclazole$_{HOMO}$:NADP$^+_{LUMO}$	−3.4 (−78)
NADP$^+_{HOMO}$:tricyclazole$_{LUMO}$	−14 (−320)
tricyclazole$_{HOMO}$:NADPH$_{LUMO}$	−9.6 (−220)
tricyclazole$_{LUMO}$:NADPH$_{HOMO}$	−7.3 (−170)

The gas phase energy gaps between all HOMO/LUMO pairs are large and indicate the lack of complete charge transfer complexes in either ternary complex. Tricyclazole is not reduced by NADPH (data not shown) which is consistent with a large barrier to charge transfer. The molecular orbital overlaps of the higher energy NADP$^+_{HOMO}$ pairs (NADP$^+_{HOMO}$/tricyclazole$_{LUMO}$ and NADPH$_{LUMO}$/tricyclazole$_{HOMO}$) are qualitatively similar to one another, and so comparing the remaining pairs (NADP$^+_{LUMO}$/tricyclazole$_{HOMO}$ and NADPH$_{HOMO}$/tricyclazole$_{LUMO}$) is more informative. The lower energy molecular orbital pairs are shown in Figure 6. The MO (ψ) phases of the tricyclazole$_{HOMO}$ and the NADP$^+_{LUMO}$ are not favorably aligned. A lobe of the NADP$^+_{LUMO}$ lies equally over opposite phased lobes of the tricyclazole$_{HOMO}$ leading to an unfavorable interaction. Conversely, there is an overall favorable phase complement between the tricyclazole$_{LUMO}$ and the NADPH$_{HOMO}$ which is qualitatively consistent with the enhanced binding of tricyclazole to 3HNR·NADPH. In effect, the NADPH *pro-S* hydrogen atom (which is delivered to substrate trihydroxynaphthalene) is pointed toward the near-center of the tricyclazole triazole ring and contributes to a positive electrostatic interaction with the triazole π-electron cloud. Increasingly, researchers have documented the albeit weak non-bonded interactions between hydrogen atoms and π-bonds (Nishio *et al.*, 1995), an effect not available to the 3HNR·NADP$^+$·tricyclazole complex. The qualitative agreement between the molecular orbital overlaps of the two ligands of 3HNR in the complexes in question suggests that consideration of frontier molecular orbitals may be useful in ligand design.

Partitioning of Scytalone and U7278. U7278 and scytalone were oxidized simultaneously in the presence of 3HNR and NADP$^+$, and by measuring the net absorbance changes at several wavelengths, the individual rates for oxidation of each substrate were extracted. The ratio of these rates over a range of concentrations of NADP$^+$ was 8 ± 0.8 which when corrected for the concentrations of the two naphthol substrates, gives a partition ratio, Φ, of 95 ± 9. Within error, Φ did not change across the range of NADP$^+$ concentrations surveyed. The K_d (NADP$^+$) = 35 μM (Table 2) so the data (collected at [NADP$^+$] = 10, 20, and 100 μM) yield Φ at different ratios of the binary complex 3HNR·NADP$^+$ to free 3HNR.

Partition analysis can be an effective method for measurement of substrate specificity. By partition analysis with a substrate of known K_m (e.g., scytalone) the k_{cat}/K_m(U7278) of 3HNR may be accurately measured spectrophotometrically. The ratio [k_{cat}/K_m(U7278)]/[k_{cat}/K_m(scytalone)] will equal Φ at saturating NADP$^+$ irrespective of an ordered or random sequential mechanism (Fersht, 1984). Since Φ = 95, the ratio of [k_{cat}/K_m(U7278)]/[k_{cat}/K_m(scytalone)] and the overall specificity of 3HNR for U7278 over scytalone at high NADP$^+$ is 95-fold. This ratio allows calculation of k_{cat}/K_m(U7278) and K_m(U7278) as shown in Table 1. These independently determined k_{cat}/K_m's and K_m's are in reasonable agreement. This agreement validates the multiwavelength partition analysis as described in materials and methods which has proven to be a convenient method to measure Φ. Since the rates of reaction of the two substrates are measured in the same mixture, cumulative errors in assay conditions do not propogate into the error in Φ. In principle, one can accurately measure Φ with just one assay by multiple wavelength analysis.

Partition analysis can also help determine the kinetic mechanism in favorable cases. If the kinetic mechanism is random sequential, Φ will vary as the ratio of 3HNR·NADP$^+$/3HNR(unliganded) in the following way. If NADP$^+$ is saturating, then Φ will approach the ratio [k_{cat}/K_m(U7278)]/[k_{cat}/K_m(scytalone)]. As NADP$^+$ approaches zero, Φ will approach the ratio [K_d(scytalone)/K_d(U7278)][k_{cat}/K_m^{U7278}(NADP$^+$)]/[$k_{cat}/K_m^{scytalone}$(NADP$^+$)] (the superscripts refer to the naphthol bound to 3HNR before NADP$^+$ adds). In the case of 3HNR, this lower limit is complex and cannot be measured directly because free 3HNR cannot be saturated with naphthol in order to determine $k_{cat}/K_m^{naphthol}$(NADP$^+$). However, in the case of an ordered sequential mechanism

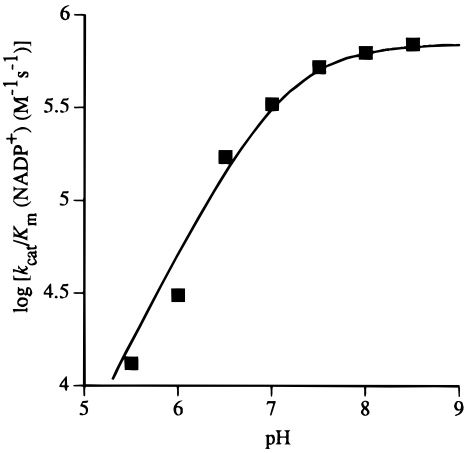

FIGURE 7: k_{cat}/K_m(NADP$^+$) for U7278 oxidation as function of pH. The solid line is the fit of the data to eq 2.

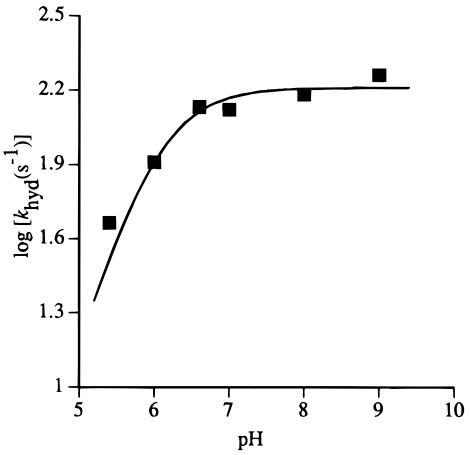

FIGURE 8: k_{hyd}(U7278) as a function of pH. The solid line is the fit of the data to eq 2.

with NADP$^+$ binding first, Φ should equal [k_{cat}/K_m(U7278)]/[k_{cat}/K_m(scytalone)] at any ratio of 3HNR·[NADP$^+$]/3HNR-(unliganded).

As noted above, Φ is invariant at NADP$^+$ concentrations less than and greater than K_d(NADP$^+$). The possibility that the limit of Φ at low NADP$^+$ concentrations {= [K_d(scytalone)/K_d(U7278)][k_{cat}/K_m^{U7278}(NADP$^+$)]/$k_{cat}/K_m^{scytalone}$(NADP$^+$)]} is coincidentally equal to the limit of Φ at high NADP$^+$ {= [k_{cat}/K_m(U7278)]/[k_{cat}/K_m(scytalone)]} cannot be excluded, in which case even a totally random sequential mechanism would show no variation of Φ with NADP$^+$ concentration. However, the partition ratio data, considered with the dramatic increases in affinity of scytalone and U7278 for 3HNR on binding of NADP$^+$ (K_d/K_m = 36 and 280 for U7278 and scytalone respectively) constitute strong evidence that an ordered sequential mechanism with nucleotide binding first predominates under physiological conditions. Such mechanisms are common for NAD(P)$^+$ dependent enzymes (Bonete *et al.*, 1990; Forte-McRobbie & Pietrusko, 1989; Wedler *et al.*, 1992).

Burst Kinetics and pH Dependence of k_{hyd} and k_{cat}/K_m(NADP$^+$). The pH dependence of k_{hyd}(U7278), the rate constant for hydride transfer from U7278 to NADP$^+$, and k_{cat}/K_m(NADP$^+$) were measured and are plotted in Figures 7 and 8, respectively. The parameters extracted from these plots are listed in Table 5. The plot of k_{cat}/K_m(NADP$^+$) suggests that deprotonation of a single ionizable group with p$K_a \approx 7$ is required for catalysis when NADP$^+$ is subsaturating. Since the affinity of 3HNR for NADP$^+$ has a similar pH dependence (data not shown), it is likely that the ionizing group is the 2′ phosphate of NADP$^+$.

Table 5: pK_a's and pH Independent Values for k_{hyd} and k_{cat}/K_m(NADP$^+$) for 3HNR-Catalyzed U7278 Oxidation

kinetic parameter	pK_a	pH independent value
k_{hyd}	6.0 ± 0.2	160 ± 9 s^{-1}
$k_{cat}/K_{m\,(NADP^+)}$[a]	7.1 ± 0.1	(7.0 ± 0.5) × 10^5 M^{-1} s^{-1}

[a] Measured at U7278 = 0.2 mM.

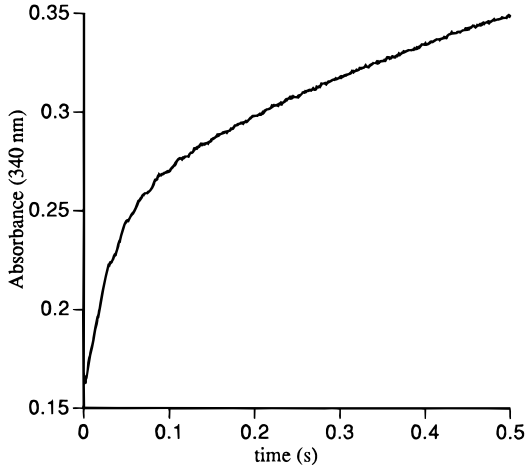

FIGURE 9: Turnover of excess U7278 and NADP$^+$ by 20 μM 3HNR in the pre-steady-state and steady-state, as measured by absorbance at 340 nm. The *y* intercept is 0.17 due to absorbance at 340 nm of substrate U7278.

The pH dependence of k_{hyd} is consistent with general base (pK_a = 6.0) assisted deprotonation of the alcohol on oxidation of the C-4 carbon by NADP$^+$. The possibility that the apparent k_{hyd} is partially or wholly limited by conformational shift of the Michaelis complex cannot be excluded by the present data. However, we believe it is unlikely that a conformational shift would have a pH dependence as that shown in Figure 8. The crystal structure of the 3HNR·NADPH·tricyclazole complex shows that 3HNR has the canonical active site feature of the short-chain dehydrogenase family, a YXXXK sequence (Andersson *et al.*, 1996a) beginning at position 178 in 3HNR. It has been postulated previously that the tyrosine in this sequence may serve as an general acid/base catalyst, as mutation of this tyrosine to phenylalanine in *Drosophila* alcohol dehydrogenase yields an inactive enzyme (Albalat *et al.*, 1992; Chen *et al.*, 1993).

It is also interesting to note that the pH 7 k_{hyd}(U7278) (132 s^{-1}) is 9 times greater than k_{cat} (14 s^{-1}) for U7278 oxidation. Hence, hydride transfer does not completely limit the rate of U7278 oxidation. We performed a pre-steady-state kinetic experiment in the presence of excess U7278 and found that there is a burst during the initial turnover (Figure 9). The burst corresponds to 23 μM substrate oxidized in the presence of 20 μM 3HNR, a stoichiometry of 1 to 1 within experimental error. These data indicate that product release limits the rate of U7278 oxidation by 3HNR.

NAD$^+$/NADP$^+$ Specificity. The kinetic parameters for U7278 oxidation with NADP$^+$ and NAD$^+$ are listed in Table 6. 3HNR shows a 770-fold preference for NADP$^+$ as measured by the relative k_{cat}/K_m for each dinucleotide. This specificity is lower than that of some other dehydrogenases; for example, isocitrate dehydrogenase from *Sulfobus acido-*

Table 6: Kinetic Parameters for 3HNR-Catalyzed U7278 Oxidation with $NADP^+$ or NAD^+ at pH 7.0

nucleotide	K_m (mM)	k_{cat}/Km ($_M^{-1}$ s^{-1})	k_{cat} (s^{-1})
NAD^+	3.0 ± 0.4	390 ± 35	1.2 ± 0.1
$NADP^+$	0.025 ± 0.003	(3.0 ± 0.2) × 10^5	7.5 ± 0.3

caldarius has a 1400-fold specificity for $NADP^+$ over NAD^+ (Wakagi *et al.*, 1993). In the crystal structure of 3HNR there is a single positively charged residue, Arg39, close to the 2′-phosphate of NADPH (Andersson *et al.*, 1996a).

Conclusions. The amino acid sequence and tertiary structure of 3HNR fit the criteria for membership in the short-chain dehydrogenase (SDR) superfamily of enzymes (Andersson *et al.*,1996a; Jornvall *et al.*, 1995). 3HNR is 60% homologous in amino acid sequence to *ver1*, a SDR enzyme involved in the biosynthesis of aflatoxin A from versicolorin A. We have shown through partition and inhibition analysis that the kinetic mechanism of 3HNR is a preferred ordered sequential mechanism with nucleotide binding first and leaving last. The rate constant for hydride transfer is 9 times greater than the overall k_{cat} at pH 7.0, and the kinetic trace of U7278 oxidation shows a burst phase in the initial turnover, so product release/isomerization steps may limit the rate of catalysis.

The pH dependences of the kinetic parameters of naphthol oxidation by 3HNR (this work) are similar to that of the SDR *Drosophila* alcohol dehydrogenase (Chen *et al*., 1993), which also suggest that a single deprotonated enzymic residue of p$K_a \approx 7$ is required for catalysis. This residue has been proposed to be a tyrosine absolutely conserved in SDR's; mutation of this tyrosine to phenylalanine results in a catalytically inactive enzyme (Chen *et al*., 1993). A proposed mechanism for general acid/base catalysis by the conserved tyrosine depicts direct shuttling of a proton between the conserved tyrosine and a conserved lysine four residues toward the N-terminus (Mckee *et al.*, 1991). In the structure of the 3HNR·NADPH·tricyclazole complex, the conserved ϵ NH_3 of Lys182 is 4.5 Å away from the hydroxyl of Tyr178 (Andersson *et al.*, 1996a), which is too great a distance for direct proton transfer. It is suggested by the structure, as shown in Figure 3, that the 2′-OH of the NADP(H) cofactor could mediate the proton transfer; alternatively Lys182 may serve only to lower the pK_a of Tyr 178.

The kinetics of tricyclazole inhibition are simpler than initially reported (Viviani *et al.*, 1993): inhibition is competitive with respect to the naphthol substrate and there is a single binding site per active site. Our studies also show that oxidized and reduced NADP(H) modulate inhibitor binding and that the inhibitor binds with the preferences 3HNR·NADPH > 3HNR·$NADP^+$ > 3HNR (unliganded). A similar progression of binding affinities is seen in methotrexate (MTX) binding to dihydrofolate reductase (DHFR), but the differences are much greater. K_i for MTX·NADPH·DHFR is estimated to be 1.5×10^{-11} M, compared to a K_i for MTX·$NADP^+$·DHFR of 1.3×10^{-6} M representing a difference of 5 orders of magnitude (Birdsall *et al.*, 1980). In contrast, 3HNR·NADP(H)·tricyclazole shows only a 36-fold increase in affinity upon reduction of the cofactor (Table 3). We believe this subtle but significant increase in affinity can be rationalized in terms of molecular orbital interactions; consideration of such interactions may be generally useful as a means to design new ligands of greater affinity when structures of ligand:protein complexes are available.

ACKNOWLEDGMENT

We thank Mike Picollelli and Rand Schwartz for purifying 3HNR and Lynn Abell, Alan Rendina, and Wendy Taylor for helpful discussions.

SUPPORTING INFORMATION AVAILABLE

Plots of tricyclazole inhibition as a function of NADPH and phenanthrenequinone; a plot of the titration of the 3HNR active-site with tricyclazole: and a figure of the pair of HOMOs/LUMOs of NADP(H) and tricyclazole that is not displayed in the text (4 pages). Ordering information is given on any current masthead page.

REFERENCES

Albalat, R., Duatre, G., & Atrian, S. (1992) *FEBS Lett. 308*, 235−239.

Andersson, A., Jordan, D., Schneider, G., & Lindqvist, Y. (1996a) *Structure 4*, 1161−1170.

Andersson, A., Jordan, D., Schneider, G., Valent, B., & Lindqvist, Y. (1996b) *Proteins: Struct., Funct. Genet. 24*, 525−527.

Birdsall, B., Burgen, A. S. V., & Roberts, G. C. K. (1980) *Biochemistry 19*, 3723−3731.

Bonete, M. J., Comacho, M. L., & Cadenas, E. (1990) *Biochim. Biophys. Acta 1041*, 305−310.

Chen, Z., Jiang, J. C., Lin, Z.-G., Lee, W. R., Baker, M. E., & Chang, S. H. (1993) *Biochemistry 32*, 3342−3346.

Chumley, F. G., & Valent, B. (1990) *Mol. Plant−Microbe Interact. 3*, 135−143.

Dewar, S. J. M. (1983) *J. Mol. Struct. 100*, 41−50.

Fersht, A. (1984) *Enzyme Structure and Mechanism*, W. H. Freeman and Company, New York.

Forte-McRobbie, C., & Pietrusko, R. (1989) *Biochem. J. 261*, 935−943.

Genetic Computer Group (1994) in *Program Manual for the Wisconsin Package, Version 8*, Genetics Computer Group, Madison, WI.

Howard, R. J., & Ferrari, M. A. (1989) *Exp. Mycol. 13*, 403−418.

Jornvall, H., Persson, B., Krook, M., Atrian, S., Gonzalez-Duarte, R., Jeffrey, J., & Ghosh, D. (1995) *Biochemistry 34*, 6003−6013.

Mckee, J. S. M., Winberg, J.-O., & Petterson, G. (1991) *Biochem. Int. 26*, 879−885.

Naumann, R., & Kayser, D. (1978) *Bioelectrochem. Bioenerg. 5*, 252−263.

Nishio, M., Umezawa, Y., Hirota, M., & Takeuchi, Y. (1995) *Tetrahedron 51*, 8665−8701.

Segel, I. H. (1975) *Enzyme Kinetics*, John Wiley & Sons, New York.

Viviani, F. (1990) Ph.D. Thesis, University of Paris.

Viviani, F., Gaudry, M., & Marquet, A. (1991) in *Bioorganic Chemistry in Healthcare and Technology* (Alderweireldt, F. C., & Pandit, U. K., Eds.), Plenum Press, New York.

Viviani, F., Gaudry, M., & Marquet, A. (1992) *New J. Chem. 16*, 81−87.

Viviani, F., Vors, J. P., Gaudry, M., & Marquet, A. (1993) *Bull. Soc. Chem. Fr. 136*, 395−404.

Wakagi, T., Eguchi, H., & Oshima, T. (1993) *Life Sci. Adv.: Biochem. 12*, 57−66.

Wedler, F. C., Ley, B. W., Spencer, S. L., Rembish, S. J., & Kushmaul, D. L. (1992) *Biochim. Biophys. Acta 1119*, 247−249.

Wheeler, M. H., (1982) *Exp. Mycol. 6*, 171−179.

BI962355U